

## Supporting Information:

### The semiquinone radical anion of 1,10-phenanthroline-5,6-dione: synthesis and rare earth coordination chemistry.

James R. Hickson,<sup>a,b</sup> Samuel J. Horsewill,<sup>a</sup> Jake McGuire,<sup>a</sup> Claire Wilson,<sup>a</sup> Stephen Sproules\*<sup>a</sup>  
and Joy H. Farnaby\*<sup>a</sup>

<sup>a</sup> School of Chemistry, WestCHEM, University of Glasgow, Glasgow, UK.

<sup>b</sup> Department of Chemistry, Imperial College London, South Kensington, London, UK.

## Contents

<b>General Experimental:</b> .....	2
<b>Spectroscopic Data for complexes 1-4, [K]<sup>+</sup>[pd]<sup>•-</sup> and [Y(hfac)<sub>3</sub>(THF)<sub>2</sub>]:</b> .....	7
<b>Additional Crystallographic Data:</b> .....	17
<b>Computational details:</b> .....	18
<b>References</b> .....	26

## General Experimental:

### General Experimental Considerations

All air-sensitive manipulations were carried out in an MBraun glovebox ( $O_2$  and  $H_2O$  <1 ppm) or by using standard Schlenk techniques under  $N_2$ . All glassware was dried at 130 °C overnight prior to use. Filter cannulas were prepared using Whatman 25 mm glass microfiber filters and were pre-dried at 130 °C overnight. Dry solvents were obtained using an Innovative Technology Inc. Pure Solv 400-5-MD solvent purification system (activated alumina columns). Solvents were sparged with  $N_2$  and stored in ampoules over activated molecular sieves under  $N_2$ . Deuterated benzene and THF were dried by refluxing over K. Deuterated acetonitrile was dried by refluxing over  $CaH_2$ . Dry deuterated solvents were degassed by three freeze-thaw cycles, vacuum distilled, and kept in ampoules in the glovebox under  $N_2$ .

The following starting materials were prepared according to literature procedures:  $CoCp_2$ ,<sup>1</sup>  $K(hfac)$ ,  $Y(OTf)_3$  and  $pd$  were synthesised according to the methods given in our recent publication.<sup>2</sup> 1,2,3,4-tetramethylcyclopentadiene ( $HCp^{tet}$ ) was purchased from Aldrich and degassed by three freeze-thaw cycles before being deprotonated by reaction with  $KN''$  to give  $K(Cp^{tet})$ .

### Physical Methods

$^1H$  NMR data were recorded on an AVIII 400 MHz instrument and were referenced internally to the appropriate residual protio-solvent and are reported relative to tetramethylsilane ( $\delta = 0$  ppm).  $^{19}F$  and  $^{19}F\{^1H\}$  NMR spectra were recorded on a Bruker AVIII 400 MHz spectrometer and were referenced to  $CFCl_3$  ( $\delta = 0$  ppm). All spectra were recorded at a constant temperature of 293 K. Coupling constants ( $J$ ) are reported in hertz (Hz). Standard abbreviations indicating multiplicity were used as follows: m = multiplet, d = doublet, t = triplet, s = singlet.

UV/vis/NIR spectra were collected using a Shimadzu UV-3600 UV/vis/NIR spectrometer using anhydrous solvents, which were filtered through Celite® prior to use. ATR-IR spectra were collected using either a Shimadzu IRAffinity-1S or a Shimadzu FTIR 8400S spectrometer. Abbreviations indicating strength of bands were used as follows: s = strong, m = medium, w = weak.

Crystallographic data for single crystals of  $[\text{CoCp}_2]^+[\text{C}_{12}\text{H}_7\text{N}_2\text{O}_2]^-$  were collected by the EPSRC UK National Crystallography Service at 100 K using a Rigaku AFC12 goniometer, mounted at the window of a FR-E+ SuperBright molybdenum rotating anode generator, and equipped with a (HG) Saturn724+ detector. Single-crystal structure data for  $[\text{CoCp}_2]^+[\text{pd}]^{\bullet-}$  **1** were collected on a Bruker D8 VENTURE diffractometer equipped with a Photon II CMOS detector, with an Oxford Cryosystems N-Helix device mounted on an I $\mu$ S 3.0 (dual Cu and Mo) microfocus sealed tube generator. Data were collected at 150 K using Mo-K $\alpha$  radiation ( $\lambda = 0.71073 \text{ \AA}$ ). CCDC numbers 1854232-1854233 contain the crystallographic information for this paper.

Elemental analysis was performed either at Strathclyde University (for  $[\text{K}]^+[\text{pd}]^{\bullet-}$ , **1** and **3**) or at London Metropolitan University (for **2** and **4**). A combustible (Tungstic Oxide) was used to ensure complete combustion of the samples.

X-band EPR spectra were collected on a Bruker ELEXSYS E500 spectrometer and simulations were performed using Bruker's Xsophe software package.<sup>3</sup>

### **S1. Synthesis of $[\text{K}]^+[\text{pd}]^{\bullet-}$**

A solution of pd (0.50 g, 2.38 mmol) and 18-crown-6 (0.72 g, 2.73 mmol, 10% excess) in THF (15 mL) was added to a  $-78 \text{ }^\circ\text{C}$  cooled suspension of KH (0.095 g, 2.38 mmol) in THF (10 mL), slowly turning deep purple. The suspension was allowed to warm to room temperature with stirring and stirred for 3 h. The solution was filtered via filter cannula, Et<sub>2</sub>O (15 mL) added and the mixture allowed to stand at room temperature for 48 h, whereupon excess 18-crown-6 crystallised. The solution was filtered via filter cannula and the solvents removed in vacuo, giving pale brown solids, which regenerated a deep purple colour when dissolved in THF (0.63 g, 1.23 mmol, 45% yield). Anal. Calcd. For C<sub>24</sub>H<sub>30</sub>N<sub>2</sub>O<sub>8</sub>K: C, 56.13%; H, 5.89%; N, 5.45%. Found: C, 59.76%; H, 5.80%; N, 6.53%. IR (ATR): 1699 (m) 1650 (w) 1636 (w) 1601 (m) 1558 (s) 1432 (m) 1416 (m) 1345 (m) 1285 (s) cm<sup>-1</sup>.  $\lambda_{\text{max}}$  (THF)/nm: 547.

### **S2. Alternative synthesis of $[\text{K}]^+[\text{pd}]^{\bullet-}$**

To a suspension of KH (8.5 mg, 0.21 mmol) in DME (1 mL) in a vial, a solution of pd (0.045 g, 0.21 mmol) in DME (5 mL) was added at room temperature with stirring. The yellow suspension was stirred for 20 h, whereupon the suspension had changed colour to deep purple. The pale yellow solution was decanted, and the purple solids dried in vacuo to give

[K]<sup>+</sup>[pd]<sup>-</sup> (0.022 g). IR (ATR): 1568 (s) 1518 (m,  $\nu_{\text{CO}}$ ) 1504 (m) 1450 (m) 1412 (m) 1393 (w), 1294 (w), 1260 (w), 1175 (w)  $\text{cm}^{-1}$ .

### S3. Synthesis of [CoCp<sub>2</sub>]<sup>+</sup>[pd]<sup>-</sup> **1**

To a -78 °C suspension of pd (0.22 g, 1.0 mmol) in THF (5 mL), a solution of CoCp<sub>2</sub> (0.21 g, 1.1 mmol, 10% excess) in THF (5 mL) was added dropwise over 10 m, immediately giving a deep purple solution. The reaction was allowed to warm to room temperature with stirring, and stirred for 1 h. THF was removed *in vacuo*, and the dark purple solids washed with toluene (3 x 5 mL) and hexane (2 x 5 mL). The product was dried *in vacuo*, giving [CoCp<sub>2</sub>]<sup>+</sup>[pd]<sup>-</sup> as a deep purple powder (0.37 g, 0.93 mmol, 93% yield). Crystals of **1** suitable for X-ray diffraction were grown from a saturated MeCN solution at -35 °C over 14 days. Single crystals of [CoCp<sub>2</sub>]<sup>+</sup>[C<sub>12</sub>H<sub>7</sub>N<sub>2</sub>O<sub>2</sub>]<sup>-</sup>, a decomposition product of **1**, which were suitable for X-ray diffraction were obtained by diffusion of hexane vapour into acetonitrile solution over 14 days. <sup>1</sup>H NMR (CD<sub>3</sub>CN):  $\delta$  5.67 (10H, s, CoCp<sub>2</sub>) ppm. IR(ATR): 1575 (m), 1561 (s), 1511 (s,  $\nu_{\text{CO}}$ ), 1486 (s), 1446 (m), 1413 (m), 1402 (s)  $\text{cm}^{-1}$ . UV-vis (THF)  $\lambda_{\text{max}}/\text{nm}$  ( $\epsilon/\text{M}^{-1} \text{cm}^{-1}$ ): 401 (3 230), 560 (3 830). Anal. Calcd. for C<sub>22</sub>H<sub>16</sub>N<sub>2</sub>O<sub>2</sub>Co: C, 66.17%; H, 4.04%; N, 7.02%. Found: C, 66.19%; H, 3.96%; N, 7.46%.

### S4. Synthesis of [CoCp<sup>tet</sup><sub>2</sub>]<sup>+</sup>[pd]<sup>-</sup> **2**

A suspension of CoCl<sub>2</sub> (0.102 g, 0.786 mmol) in THF (10 ml) was added slowly to a suspension of K(Cp<sup>tet</sup>) (0.253 g, 1.58 mmol) in THF (5 ml) at -78 °C, to give a dark brown solution with suspended solids. The solution was slowly filtered *via* filter cannula onto a suspension of pd (0.133 g, 0.633 mmol) in THF (5 ml) at -78 °C, evolving a purple precipitate under a dark blue solution. The THF solution was filtered away *via* filter cannula, and the solids washed with THF (3 x 5 ml) and dried *in vacuo* to give [CoCp<sup>tet</sup><sub>2</sub>]<sup>+</sup>[pd]<sup>-</sup> as a rich purple solid (0.199 g, 0.389 mmol, 61% yield with respect to pd). <sup>1</sup>H NMR (CD<sub>3</sub>CN):  $\delta$  1.74 (12H, s, Cp-(CH<sub>3</sub>)<sub>2</sub><sup>1</sup>),  $\delta$  1.82 (12H, s, Cp-(CH<sub>3</sub>)<sub>2</sub><sup>2</sup>),  $\delta$  4.76 (2H, s, CoCp<sup>t</sup><sub>2</sub>) ppm. IR(ATR): 1668 (w), 1574 (w), 1558 (s), 1508 (w,  $\nu_{\text{CO}}$ ), 1491 (s), 1443 (s), 1402 (m), 1381 (m), 1358 (w), 1285 (w), 1115 (w), 1067 (m), 1026 (s)  $\text{cm}^{-1}$ . UV-vis (MeCN)  $\lambda_{\text{max}}/\text{nm}$  ( $\epsilon/\text{M}^{-1} \text{cm}^{-1}$ ): 397 (3 261), 548 (2 867). Anal. Calcd. for C<sub>30</sub>H<sub>32</sub>N<sub>2</sub>O<sub>2</sub>Co: C, 70.44%; H, 6.31%; N, 5.48%. Found: C, 70.22%; H, 6.15%; N, 5.64%.

### S5. Synthesis of [Y(hfac)<sub>3</sub>(THF)<sub>2</sub>]

Y(OTf)<sub>3</sub> (0.64 g, 1.18 mmol) was suspended in THF (5 mL) and cooled to -78 °C. With stirring, a solution of K(hfac) (0.88 g, 3.55 mmol) in THF (5 mL) was added. The resultant suspension was warmed to room temperature, and stirred for 16 h. THF was removed *in vacuo*, and the off-white solids extracted into toluene (2 x 10 mL). Toluene was removed *in vacuo*, and the solids washed with hexane (2 x 5 mL) to give [Y(hfac)<sub>3</sub>(THF)<sub>2</sub>] as a low melting off-white solid (0.76 g, 0.89 mmol, 75% yield). <sup>1</sup>H NMR (C<sub>6</sub>D<sub>6</sub>): δ 1.16 (8H, s, THF-CH<sub>2</sub>) 3.59 (8H, s, THF-CH<sub>2</sub>) 6.28 (3H, s, hfac-CH) ppm. <sup>19</sup>F{<sup>1</sup>H} NMR (C<sub>6</sub>D<sub>6</sub>): δ -76.68 (s, hfac-CF<sub>3</sub>) ppm. IR(ATR): 1668 (w), 1649 (s), 1612 (w), 1558 (w), 1531 (m), 1474 (s), 1250 (s), 1194 (s), 1134 (s), 1101 (m), 1022 (m) cm<sup>-1</sup>. Accurate elemental analysis was not possible due to the low-melting nature of the compound.

### S6. Synthesis of [CoCp<sub>2</sub>]<sup>+</sup>[Y(hfac)<sub>3</sub>(N,N'-pd)]<sup>-</sup>

To a schlenk containing a purple solution of [CoCp<sub>2</sub>]<sup>+</sup>[pd]<sup>-</sup> (0.16 g, 0.40 mmol) in MeCN (10 mL), a solution of [Y(hfac)<sub>3</sub>(THF)<sub>2</sub>] (0.34 g, 0.40 mmol) in MeCN (5 mL) was added at room temperature with stirring. An immediate colour change from purple to dark green was observed. The green solution was stirred for 12 h, filtered *via* filter cannula and MeCN removed *in vacuo*. The green solids were washed with hexane (3 x 5 mL) to give [CoCp<sub>2</sub>]<sup>+</sup>[Y(hfac)<sub>3</sub>(N,N'-pd)]<sup>-</sup> (0.29 g, 0.26 mmol, 65% yield). <sup>1</sup>H NMR (*d*<sub>8</sub>-THF): δ 5.82 (10H, s, CoCp<sub>2</sub>) 5.96 (3H, s, hfac-CH) 7.57 (1H, br, C<sup>3,8</sup>-H) 8.42 (1H, br, C<sup>4,7</sup>-H) 9.01 (1H, br, C<sup>2,9</sup>-H) ppm. <sup>19</sup>F{<sup>1</sup>H} NMR (*d*<sub>8</sub>-THF): δ -77.72 (s, hfac-CF<sub>3</sub>) ppm. IR (ATR): 1651 (s) 1579 (w) 1498 (m, ν<sub>CO</sub>) 1428 (w) 1251 (s) 1136 (s) cm<sup>-1</sup>. UV-vis (MeCN) λ<sub>max</sub>/nm (ε/M<sup>-1</sup> cm<sup>-1</sup>): 387 (6 986), 642 (2 356). Anal. Calcd. for C<sub>37</sub>H<sub>19</sub>F<sub>18</sub>N<sub>2</sub>O<sub>8</sub>CoY: C, 40.06%; H, 1.73%; N, 2.53%. Found: C, 39.80%; H, 1.71%; N, 2.90%.

### S7. Synthesis of [Co(Cp<sup>tet</sup>)<sub>2</sub>]<sup>+</sup>[Y(hfac)<sub>3</sub>(N,N'-O,O'-pd)]<sup>-</sup>

[Y(hfac)<sub>3</sub>(THF)<sub>2</sub>] (67.3 mg, 7.87x10<sup>-5</sup> mol) and [CoCp<sup>tet</sup>]<sub>2</sub><sup>+</sup>[pd]<sup>-</sup> (40.2 mg, 7.86x10<sup>-5</sup> mol) were dissolved separately in MeCN (3 ml each) and cooled to -35 °C in a nitrogen atmosphere glovebox. [Y(hfac)<sub>3</sub>(THF)<sub>2</sub>] was added slowly to [CoCp<sup>tet</sup>]<sub>2</sub><sup>+</sup>[pd]<sup>-</sup> with stirring, leading to an immediate change from a purple solution to a green suspension. The suspension was stirred for 2 h and filtered to give an emerald green solution. MeCN was removed *in vacuo* and the resultant green solids were suspended in THF. The green suspension was filtered, and THF

was removed *in vacuo* to leave green solids, which were washed with hexane (3x3 ml) and thoroughly dried *in vacuo* to leave  $[\text{Co}(\text{Cp}^{\text{tet}})_2]^+[\text{Y}(\text{hfac})_3(\text{N},\text{N}'\text{-pd})]^-$  as a green powder (79.9 mg,  $6.54 \times 10^{-5}$  mol, 83% yield).  $^1\text{H}$  NMR ( $d_8$ -THF):  $\delta$  1.79 (12H, s, Cp-(CH<sub>3</sub>)<sub>2</sub><sup>1</sup>) 1.88 (12H, s, Cp-(CH<sub>3</sub>)<sub>2</sub><sup>2</sup>) 5.02 (2H, s, CoCp<sup>t</sup><sub>2</sub>) 5.98 (3H, hfac-CH) 7.55 (C<sup>3,8</sup>-H) 8.41 (C<sup>4,7</sup>-H) 8.98 (C<sup>2,9</sup>-H) ppm.  $^{19}\text{F}\{^1\text{H}\}$  NMR ( $d_8$ -THF):  $\delta$  -77.78 (s, hfac-CF<sub>3</sub>) ppm. IR (ATR): 1653 (s) 1578 (w) 1555 (m) 1523 (m) 1504 (m,  $\nu_{\text{CO}}$ ) 1422 (w), 1389 (w), 1248 (s), 1192 (s), 1134 (s), 1099 (w), 1069 (w), 1030 (m)  $\text{cm}^{-1}$ . UV-vis (THF)  $\lambda_{\text{max}}/\text{nm}$  ( $\epsilon/\text{M}^{-1} \text{cm}^{-1}$ ): 457 (2 319), 607 (768). UV-vis (MeCN)  $\lambda_{\text{max}}/\text{nm}$ : 599. Anal. Calcd. for C<sub>45</sub>H<sub>35</sub>F<sub>18</sub>N<sub>2</sub>O<sub>8</sub>CoY: C, 44.25%; H, 2.89%; N, 2.29%. Found: C, 44.15%; H, 2.75%; N, 2.32%.

Spectroscopic Data for complexes 1-4,  $[K]^+[pd]^{*-}$  and  $[Y(hfac)_3(THF)_2]:$

NMR:

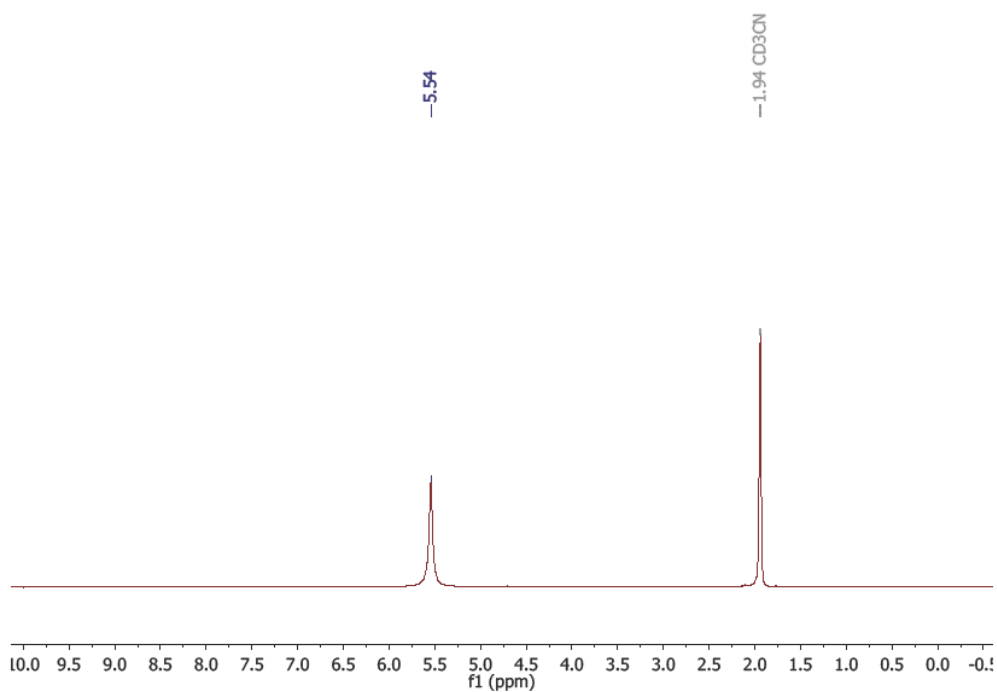


Fig. S1  $^1H$  NMR spectrum of  $[CoCp_2]^+[pd]^{*-}$  **1**, recorded in  $MeCN-d_3$  at 293 K

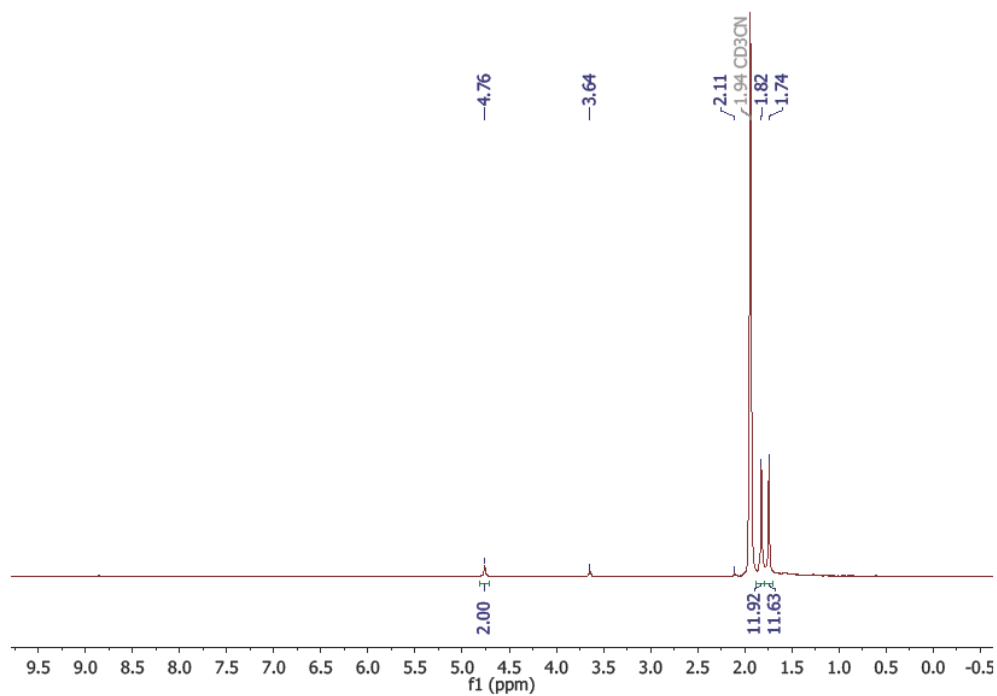
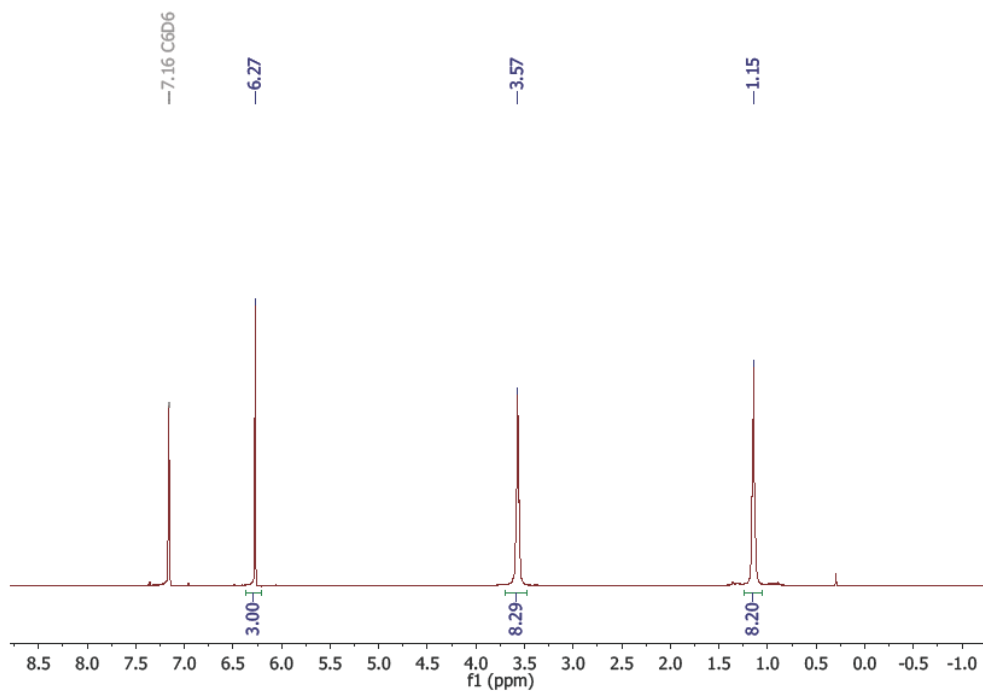
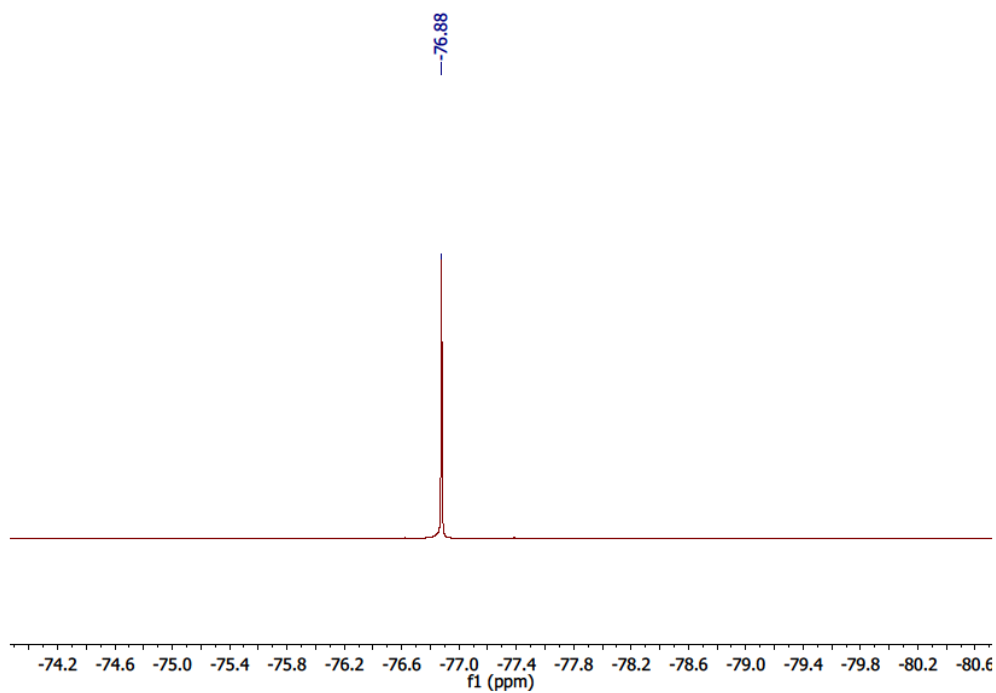


Fig. S2  $^1H$  NMR spectrum of  $[CoCp^{tet_2}]^+[pd]^{*-}$  **2**, recorded in  $MeCN-d_3$  at 293 K



**Fig. S3**  $^1\text{H}$  NMR spectrum of  $[\text{Y}(\text{hfac})_3(\text{THF})_2]$ , recorded in  $\text{C}_6\text{D}_6$  at 293 K



**Fig. S4**  $^{19}\text{F}\{^1\text{H}\}$  NMR spectrum of  $[\text{Y}(\text{hfac})_3(\text{THF})_2]$ , recorded in  $\text{C}_6\text{D}_6$  at 293 K

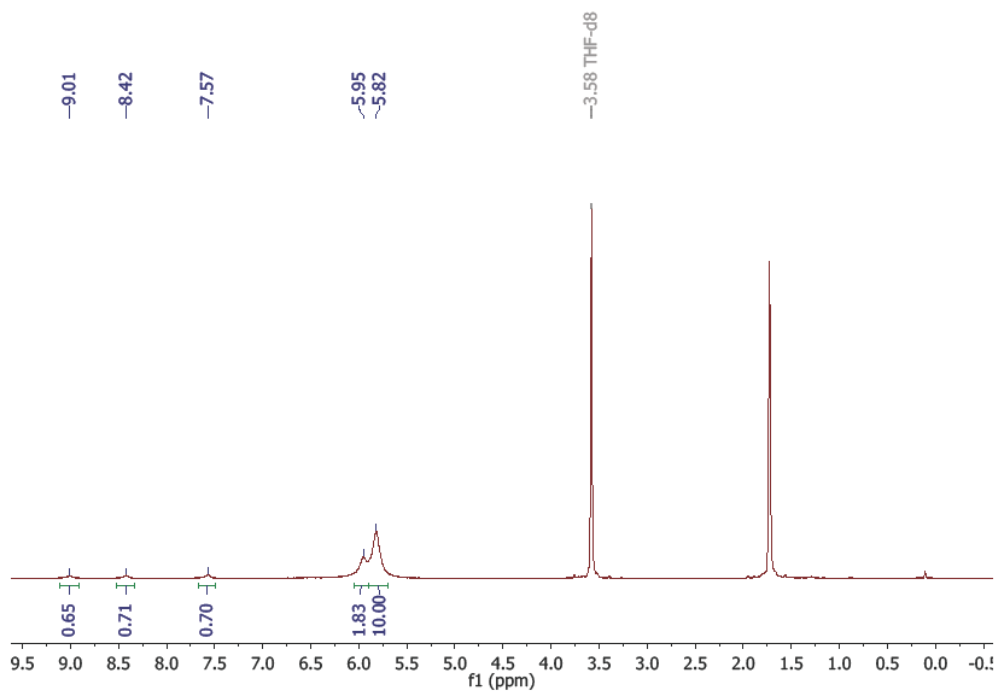


**Fig. S5**  $^1\text{H}$  NMR spectrum of  $[\text{CoCp}_2]^+[\text{Y}(\text{hfac})_3(\text{N},\text{N}'\text{-pd})]^- \mathbf{3}$ , recorded in  $\text{THF-}d_8$  at 293 K

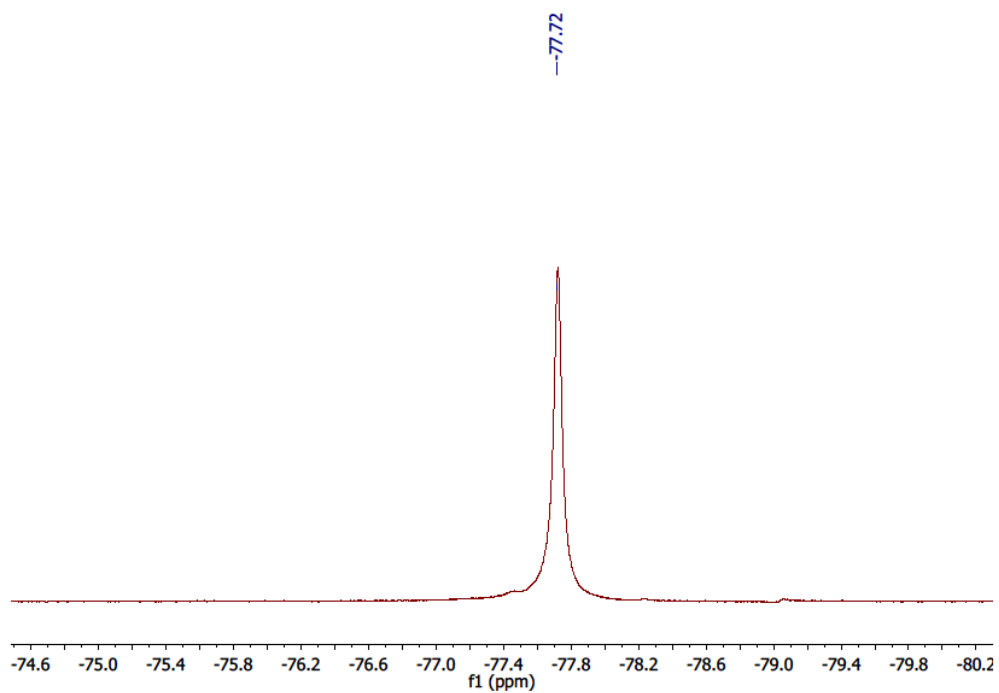


**Fig. S6**  $^{19}\text{F}\{^1\text{H}\}$  NMR spectrum of  $[\text{CoCp}_2]^+[\text{Y}(\text{hfac})_3(\text{N},\text{N}'\text{-pd})]^- \mathbf{3}$ , recorded in  $\text{THF-}d_8$  at 293 K

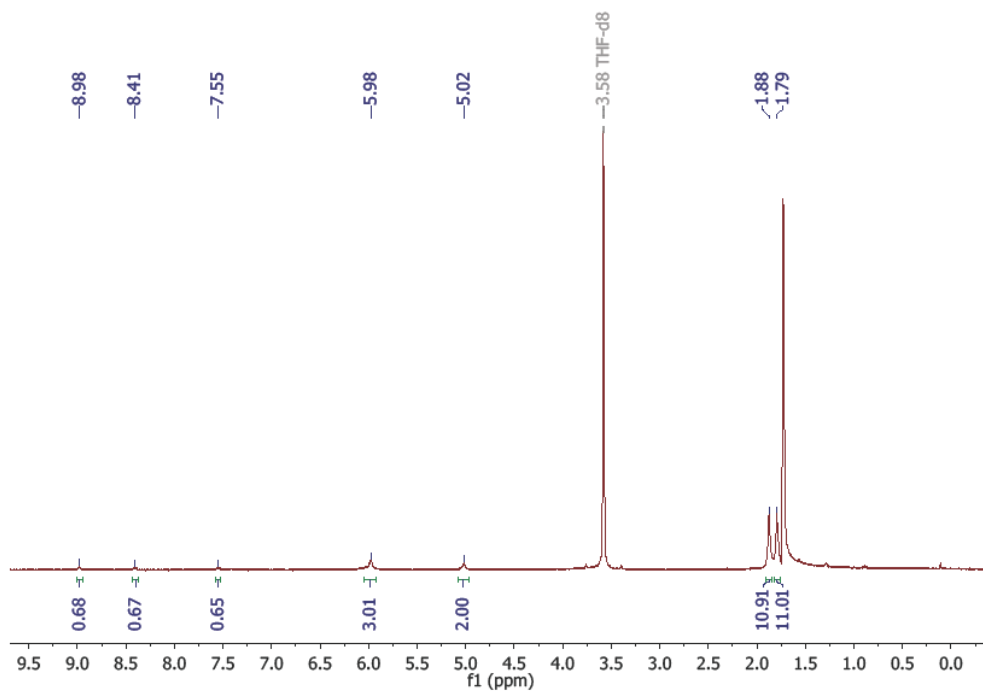


**Fig. S7**  $^1\text{H}$  NMR spectrum of  $[\text{CoCp}^{\text{tet}}_2]^+[\text{Y}(\text{hfac})_3(\text{N},\text{N}'\text{-pd})]^-$  **4**, recorded in  $\text{THF-}d_8$  at 293 K

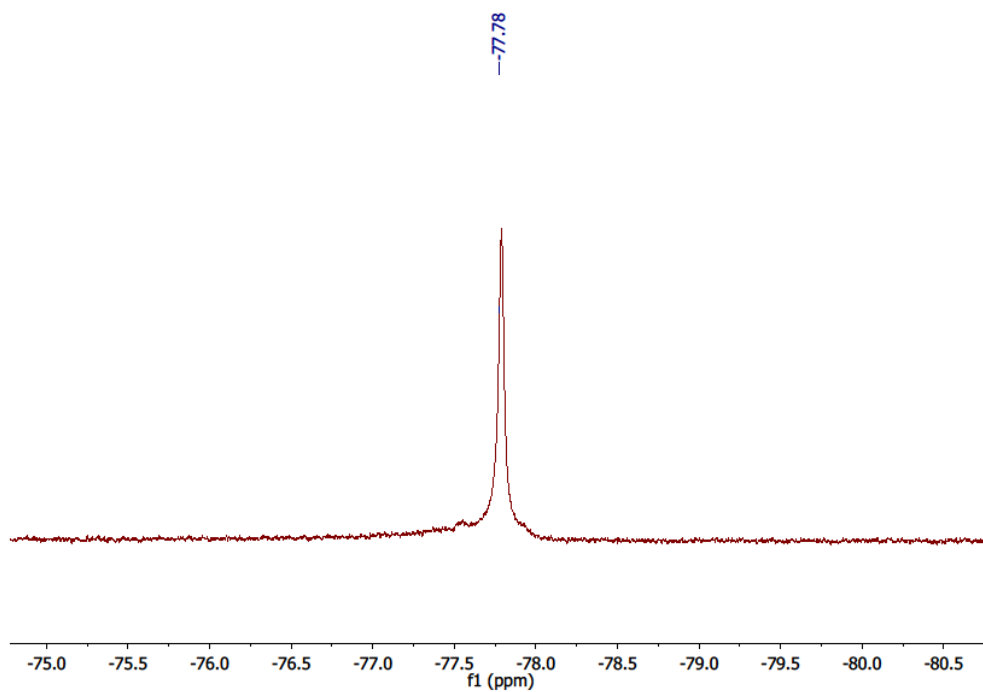


**Fig. S8**  $^{19}\text{F}$  NMR spectrum of  $[\text{CoCp}^{\text{tet}}_2]^+[\text{Y}(\text{hfac})_3(\text{N},\text{N}'\text{-pd})]^-$  **4**, recorded in  $\text{THF-}d_8$  at 293 K

IR:

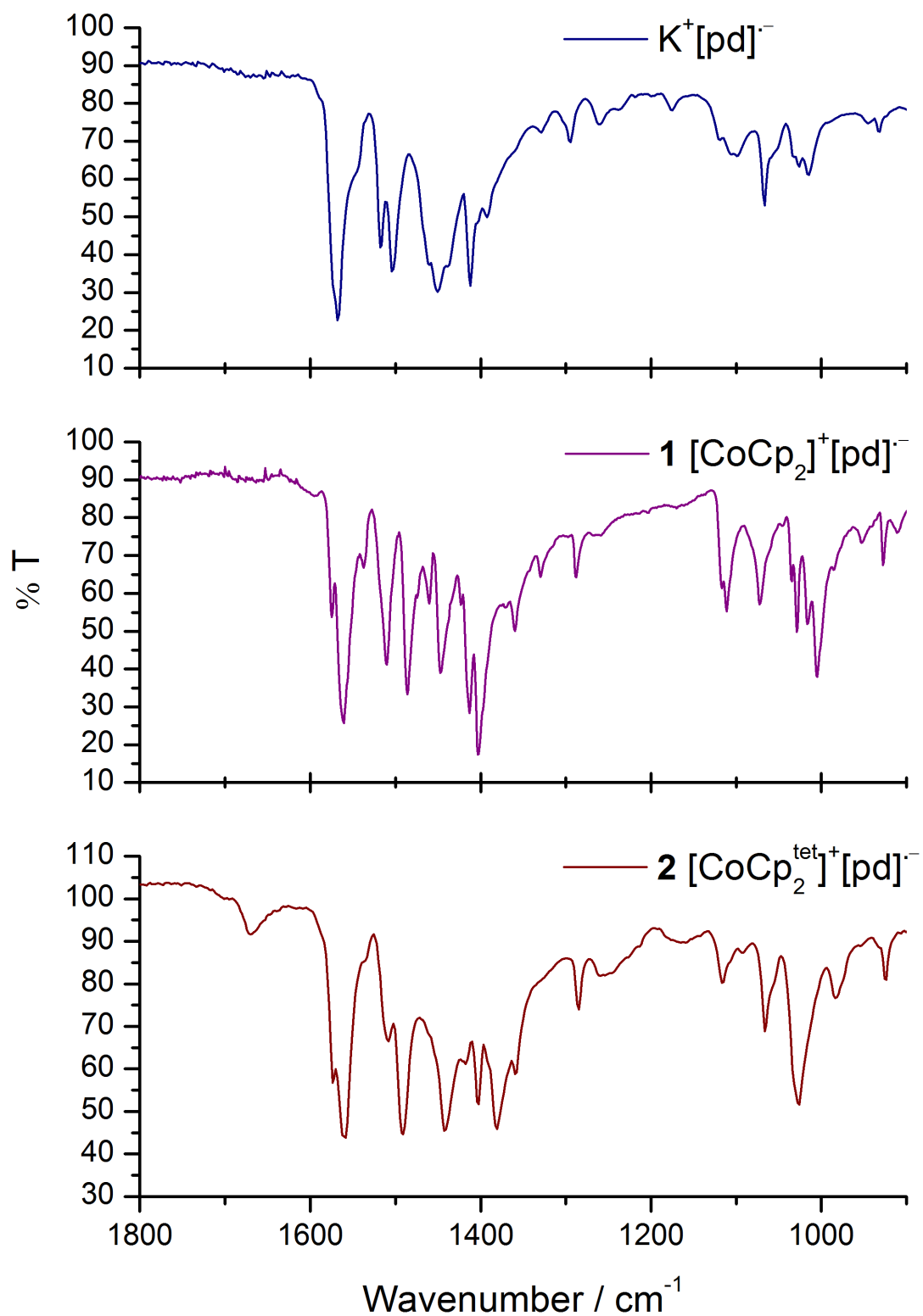


Fig. S9 ATR-IR spectra of [K]<sup>+</sup>[pd]<sup>-</sup> (ex. DME), **1** and **2**, recorded at 293 K

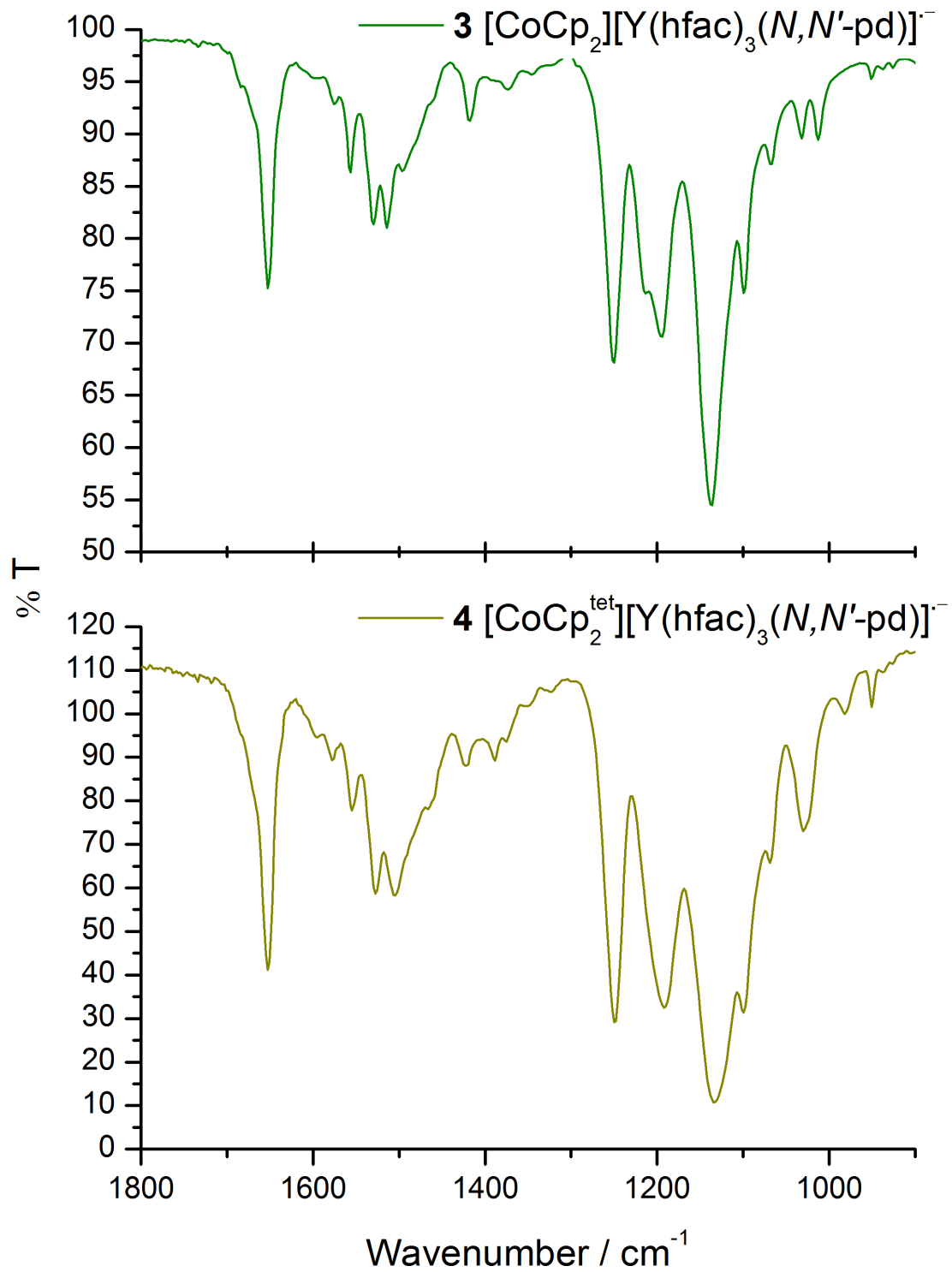
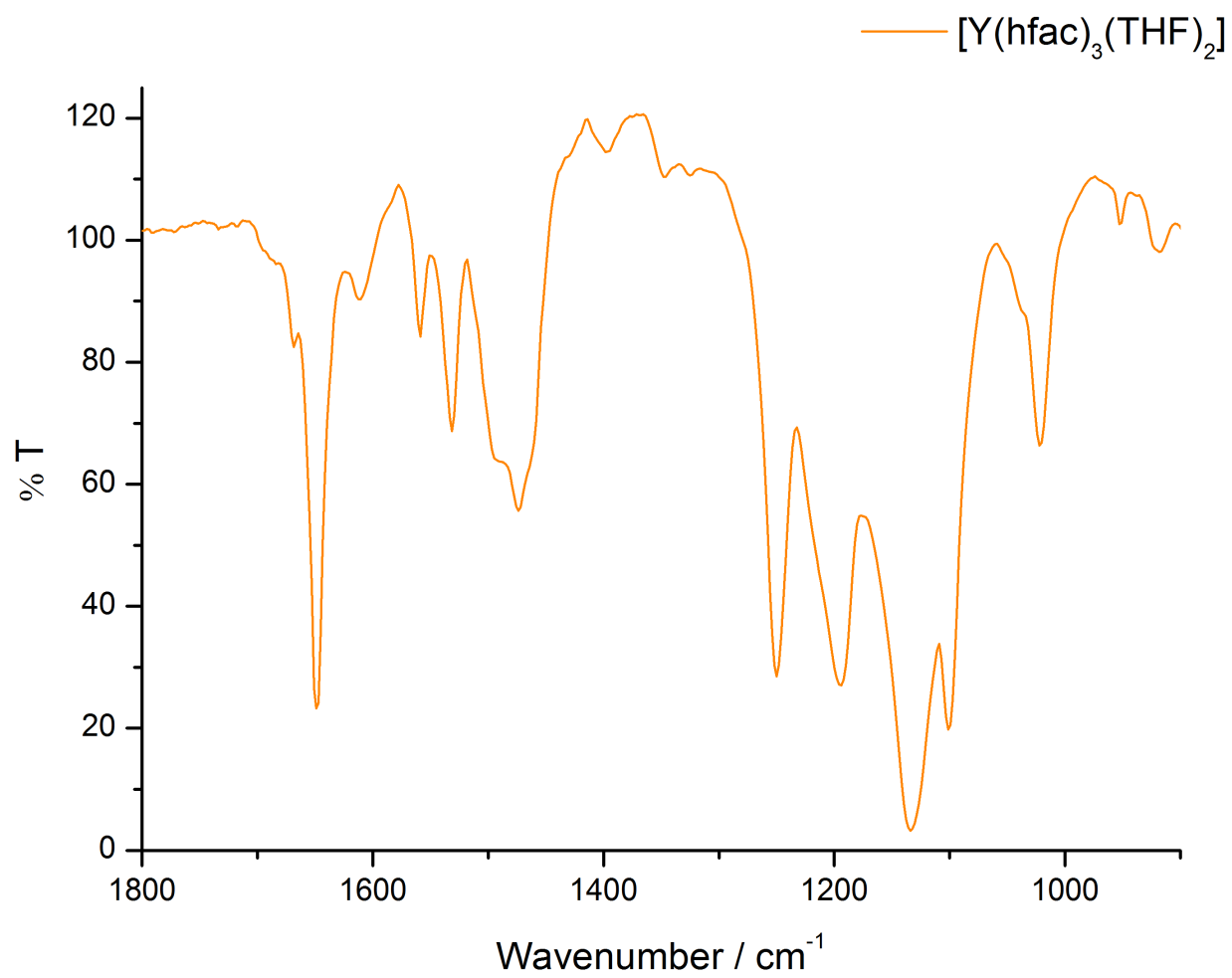
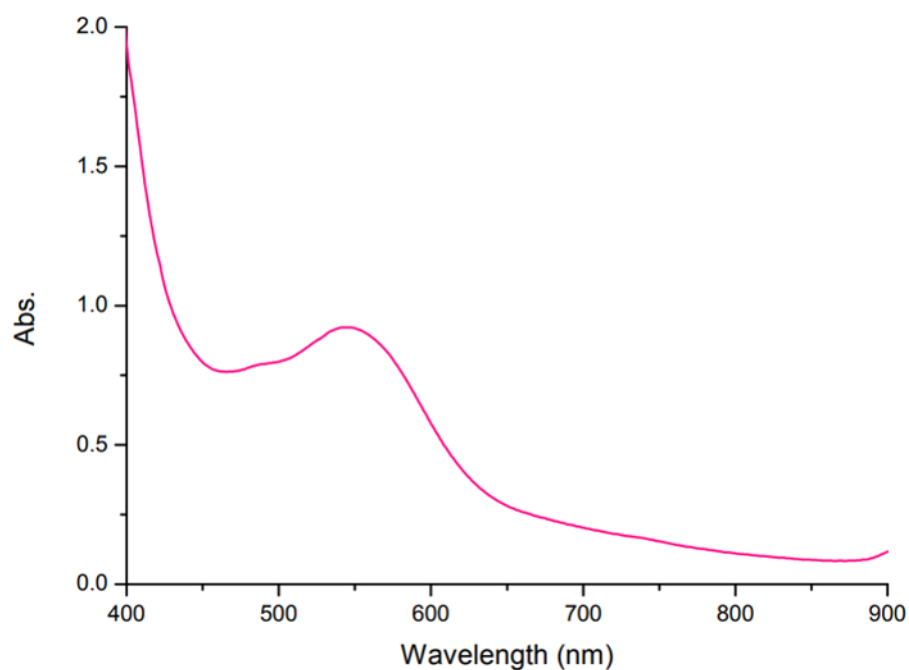


Fig. S10 ATR-IR spectra of **3** and **4**, recorded at 293 K



**Fig. S11** ATR-IR spectrum of  $[Y(hfac)_3(THF)_2]$ , recorded at 293 K

## UV-vis-NIR:



**Fig. S12** UV-vis-NIR spectrum of  $[K]^+[pd]^{*-}$ , recorded in THF at 293 K. Spectrum was collected *in situ* and yield is assumed to be non-quantitative, so no extinction coefficients have been calculated. Data is presented as recorded.

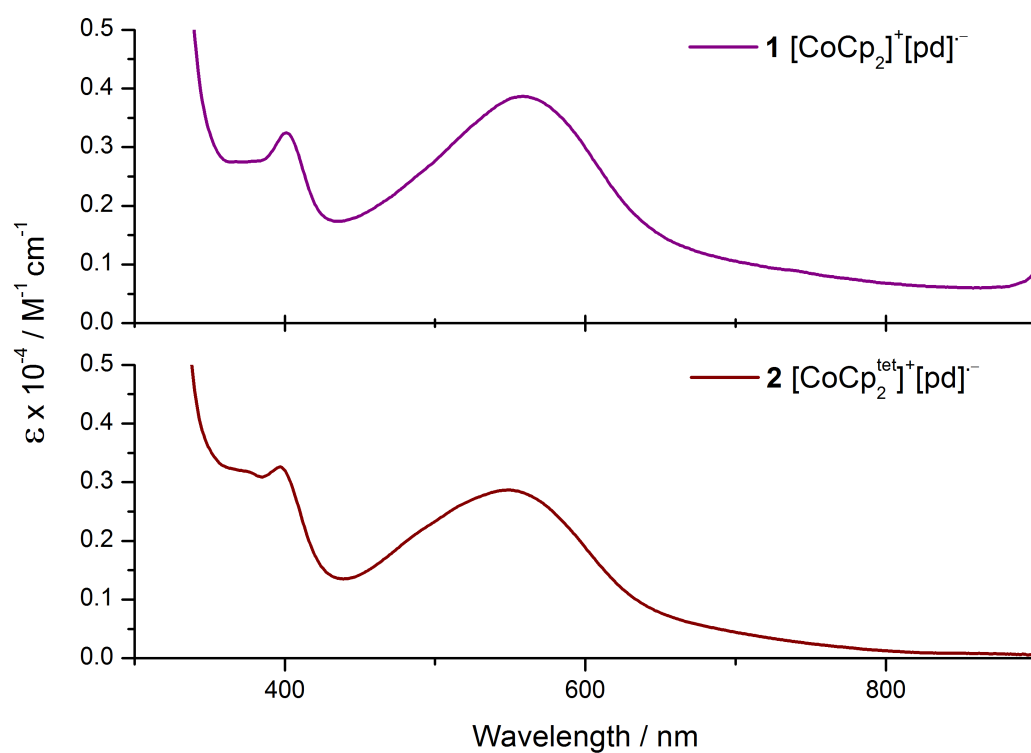


**Fig. S13** UV-vis-NIR spectra of **1** and **2**, recorded in THF and MeCN, respectively at 293 K.

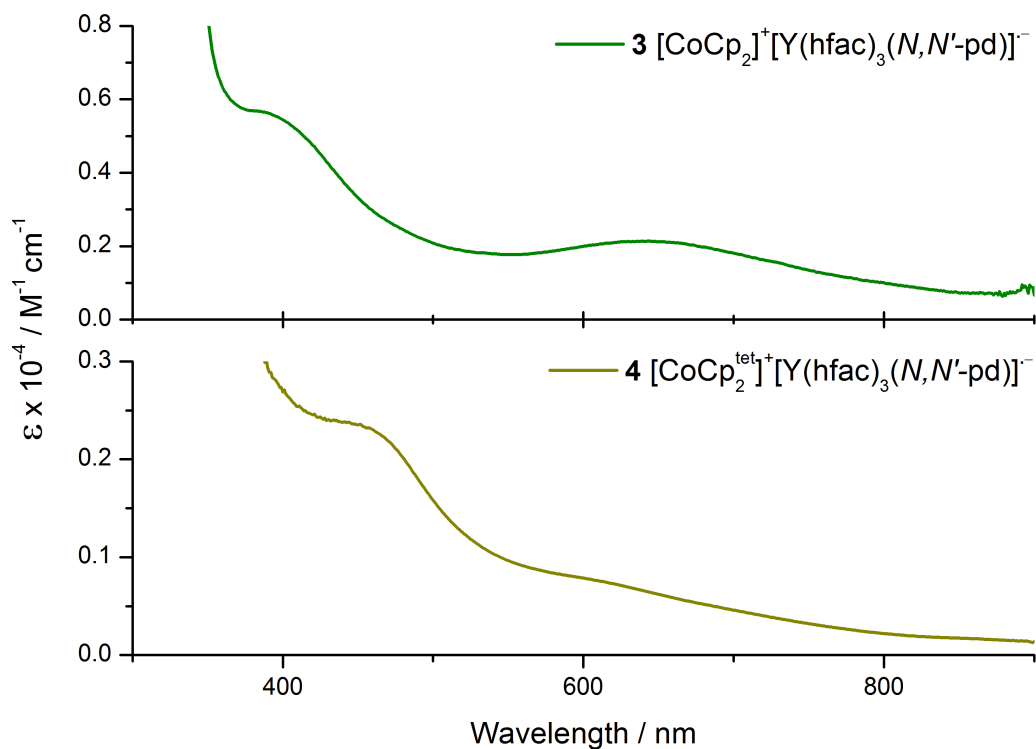


**Fig. S14** UV-vis-NIR spectra of **3**, recorded in MeCN, and **4**, recorded in THF, at 293 K.

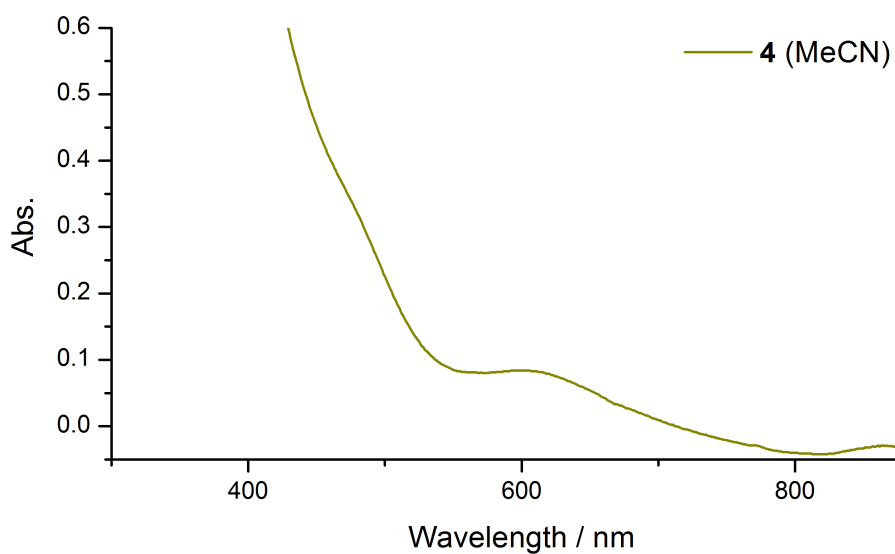


**Fig. S15** UV-vis-NIR spectrum of **4** recorded in MeCN at 293 K. Significant decomposition was observed on addition of MeCN, preventing the calculation of accurate extinction coefficients. Data is presented as recorded.

EPR:

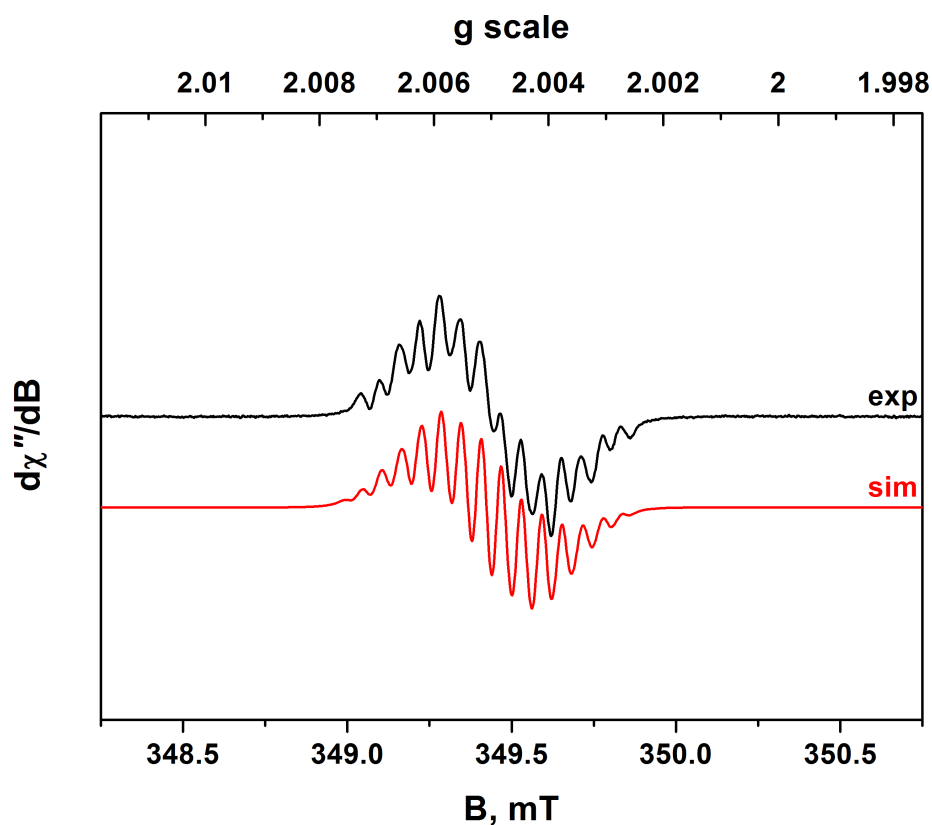


**Fig. S16** X-band EPR spectrum of  $[\text{K}]^+[\text{pd}]^{\bullet-}$  recorded in THF solution at 293 K (experimental conditions: frequency, 9.8061 GHz; power, 0.63 mW; modulation, 0.005 mT). Experimental data are represented by the black line; simulation is depicted by the red line:  $g_{\text{iso}} = 2.0051$ ;  $A_{\text{iso}}^{\text{H}1} = 1.21 \times 10^{-4} \text{ cm}^{-1}$ ;  $A_{\text{iso}}^{\text{H}2} = 1.18 \times 10^{-4} \text{ cm}^{-1}$ ;  $A_{\text{iso}}^{\text{H}3} = 0.57 \times 10^{-4} \text{ cm}^{-1}$ ;  $A_{\text{iso}}^{\text{N}} = 0.49 \times 10^{-4} \text{ cm}^{-1}$ .

## Additional Crystallographic Data:

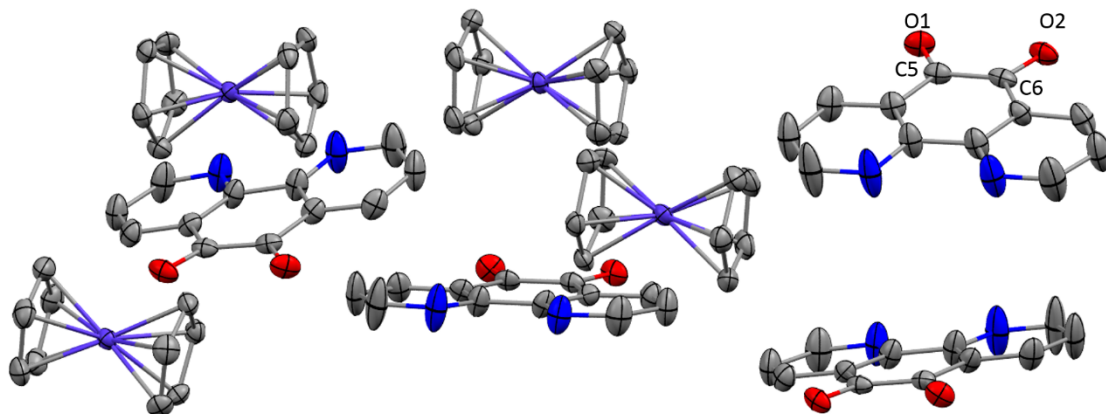


**Fig. S17** Full unit cell of the solid state crystal structure of **1**, grown from a concentrated MeCN solution at -35 °C over 14 days. Parameters are found in the main text.

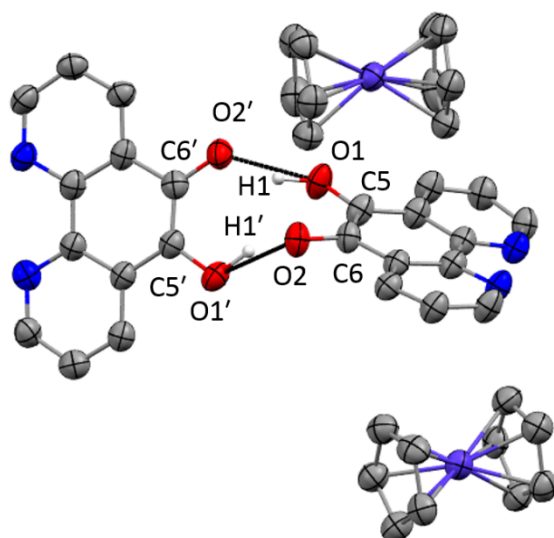


**Fig. S18** Solid state crystal structure of [CoCp<sub>2</sub>]<sup>+</sup>[C<sub>12</sub>H<sub>7</sub>N<sub>2</sub>O<sub>2</sub>]<sup>-</sup>, a decomposition product of **1**. Crystals were obtained by slow diffusion of hexane vapour into a saturated MeCN solution, over 14 days. Selected bond distances (Å): C5-C6 1.38(1) C5-O1 1.36(9) C6-O2 1.33(9) O1-H1 1.20(1) H1-O2' 1.36(2).

## Computational details:

**Calculations.** The program package ORCA was used for all calculations.<sup>4</sup> The input geometry was generated using ArgusLab, and then optimised via a spin-unrestricted DFT method employing the BP86 functional<sup>5,6</sup> with THF as solvent. Split-valence basis sets with one set of polarization functions (def2-SVP) were used for all atoms.<sup>7,8</sup> A scalar relativistic correction was applied using the zeroth-order regular approximation (ZORA) method<sup>9-11</sup> as implemented by van Wüllen.<sup>12</sup> The RI-J approximation combined with the appropriate Ahlrichs auxiliary basis set was used to speed up the calculations.<sup>13,14</sup> The conductor like screening model (COSMO) was used for all calculations.<sup>15</sup> The self-consistent field calculations were tightly converged ( $1 \times 10^{-8} E_h$  in energy,  $1 \times 10^{-7} E_h$  in the charge density, and  $1 \times 10^{-7}$  in the maximum element of the DIIS<sup>16, 17</sup> error vector). The geometry was converged with the following convergence criteria: change in energy  $< 10^{-5} E_h$ , average force  $< 5 \times 10^{-4} E_h \text{ Bohr}^{-1}$ , and the maximum force  $10^{-4} E_h \text{ Bohr}^{-1}$ . The geometry search for all complexes was carried out in redundant internal coordinates without imposing geometry constraints.

Electronic property calculations at the optimised geometry were done with the PBE0 functional.<sup>18,19</sup> The scalar relativistically recontracted ZORA-def2-TZVP(-f) were used all atoms and enhanced integration accuracy was used for yttrium (SPECIALGRIDINTACC 10).<sup>8,20</sup> Calculations employed the RIJCOSX algorithm to speed the calculation of Hartree–Fock exchange.<sup>21,22</sup> TD-DFT calculations were carried out as described by Neese and Olbrich.<sup>23</sup> The first 80 states were calculated where the maximum dimension of the expansion space in the Davidson procedure (MAXDIM) was set to 800. The full width at half maximum (FWHM) was set to  $4500 \text{ cm}^{-1}$ . Molecular orbitals and spin density maps were visualised via the programme Molekel.<sup>24</sup>

**Table S1** Geometry Optimised Coordinates for [pd]<sup>0</sup>

O	5.662008	9.038276	22.636480
O	7.007147	7.496529	20.820441
N	6.960923	6.037936	26.138556
N	8.305297	4.504151	24.329433
C	6.942792	6.437654	24.854434
C	7.676322	5.598905	23.865713
C	6.258626	7.606025	24.442963
C	7.701194	5.953514	22.495889
C	6.305871	6.783221	27.041599
C	8.970129	3.737806	23.451414
C	5.581977	8.369492	25.407133
C	8.403751	5.135505	21.597323
C	5.603675	7.955033	26.731558
C	9.050797	4.006093	22.078868
C	6.243585	8.033793	23.030908
C	7.008235	7.157306	21.998502
H	6.344053	6.424330	28.073980
H	9.466997	2.857076	23.867589
H	5.054761	9.272282	25.097262
H	8.427239	5.402997	20.540264
H	5.094124	8.516727	27.513876
H	9.606983	3.341507	21.418037

**Table S2** Geometry Optimised Coordinates for [pd]<sup>1-</sup>

O	5.646850	9.052267	22.649816
O	7.018941	7.485456	20.802233
N	6.960876	6.030598	26.168945
N	8.318913	4.477419	24.338028
C	6.956497	6.411934	24.869289
C	7.678602	5.585915	23.895618
C	6.278175	7.581418	24.419030
C	7.683225	5.974111	22.524364
C	6.303090	6.786131	27.053715
C	8.976127	3.726955	23.448455
C	5.596554	8.352540	25.384314
C	8.388894	5.155686	21.617110
C	5.605320	7.958752	26.712106
C	9.041420	4.023146	22.074904
C	6.263624	8.006677	23.010453
C	6.991544	7.174626	22.029587
H	6.329077	6.445614	28.093739
H	9.479197	2.838785	23.843445
H	5.074872	9.252169	25.054440
H	8.401648	5.440818	20.563897
H	5.089661	8.535167	27.481298
H	9.593381	3.369973	21.397439

**Table S3** Geometry Optimised Coordinates for [pd]<sup>2-</sup>

O	5.635143	9.068481	22.652770
O	7.024071	7.482635	20.782823
N	6.959529	6.025226	26.194568
N	8.331454	4.455278	24.344048
C	6.970093	6.386775	24.882564
C	7.680246	5.574335	23.924891
C	6.291055	7.567310	24.397121
C	7.667906	5.992624	22.540745
C	6.299521	6.788181	27.067096
C	8.983876	3.715626	23.446098
C	5.604426	8.343553	25.372160
C	8.380544	5.166217	21.627584
C	5.603209	7.965615	26.700159

C	9.036699	4.033642	22.067020
C	6.272812	7.993096	23.007447
C	6.987107	7.177177	22.045445
H	6.315890	6.460783	28.112729
H	9.492276	2.822344	23.825614
H	5.087117	9.241384	25.027057
H	8.384650	5.464523	20.576762
H	5.083083	8.552864	27.460169
H	9.585781	3.388489	21.377353

**Table S4** Geometry Optimised Coordinates for  $[Y(hfac)_3(pd)]^{1-}$

Y	0.372509	13.269978	11.997432
F	2.222764	8.653556	11.110616
O	1.449689	12.838755	9.940748
F	-2.902330	15.273330	8.724748
O	1.136060	11.031124	12.100088
F	-2.497343	13.993550	6.992847
F	1.977829	12.804917	6.441034
O	-1.217685	13.636564	10.274016
O	-1.081128	14.807578	13.017682
O	-1.474357	11.916085	12.543993
O	1.026858	15.424464	11.279294
F	-3.572241	11.017770	14.140474
F	3.397380	13.309999	8.030816
F	2.585289	8.901854	13.258161
F	2.617061	11.268036	7.866500
O	6.014022	13.114055	16.262523
F	0.781414	18.913101	10.723652
F	-2.780961	17.867606	13.540614
N	2.777926	13.504225	12.717806
F	-3.522859	13.171280	8.745716
F	-3.952681	10.655421	12.012240
O	3.948405	12.632185	18.072121
F	1.031769	7.522683	12.559631
N	0.759275	13.047848	14.487931
F	1.314201	17.371323	9.260911
F	-3.334194	9.003473	13.311976
F	2.600346	17.723565	11.000717
C	0.613489	9.913738	12.358928
C	2.033040	13.048465	14.962997
C	4.450301	13.322734	14.478058
C	3.107344	13.294545	14.020649
F	-3.639945	15.857626	13.400391
C	2.332291	12.834758	16.334180
F	-2.285247	16.356412	15.049576
C	3.757158	13.756719	11.839142
H	3.446051	13.919049	10.807965
C	-1.309333	16.041380	12.887293
C	-0.729872	9.643810	12.666393
H	-1.043859	8.622494	12.856048
C	-2.535735	14.017828	8.352033
C	1.134480	12.940292	8.722262
C	4.808893	13.092847	15.887166
C	0.531042	16.580943	11.379391
C	-1.187761	13.628139	9.014718
C	-0.600926	16.970382	12.110513
H	-0.913970	18.009542	12.100771
C	1.612867	8.728453	12.322268
C	5.456241	13.586406	13.526059
H	6.494453	13.612161	13.859838
C	-0.102964	13.312305	8.179573
H	-0.226810	13.347860	7.101861
C	5.111525	13.807922	12.203333
H	5.866718	14.019535	11.446566
C	-1.669811	10.681845	12.727013
C	-0.249732	12.853656	15.348820

H	-1.253988	12.880921	14.924963
C	1.247957	12.620066	17.209555
H	1.458554	12.450425	18.266437
C	3.710869	12.837179	16.848761
C	2.284243	12.581431	7.745531
C	-0.047698	12.634293	16.719811
H	-0.905083	12.479189	17.374301
C	-3.142628	10.323647	13.052624
C	1.305815	17.666694	10.589070
C	-2.514339	16.547349	13.721486

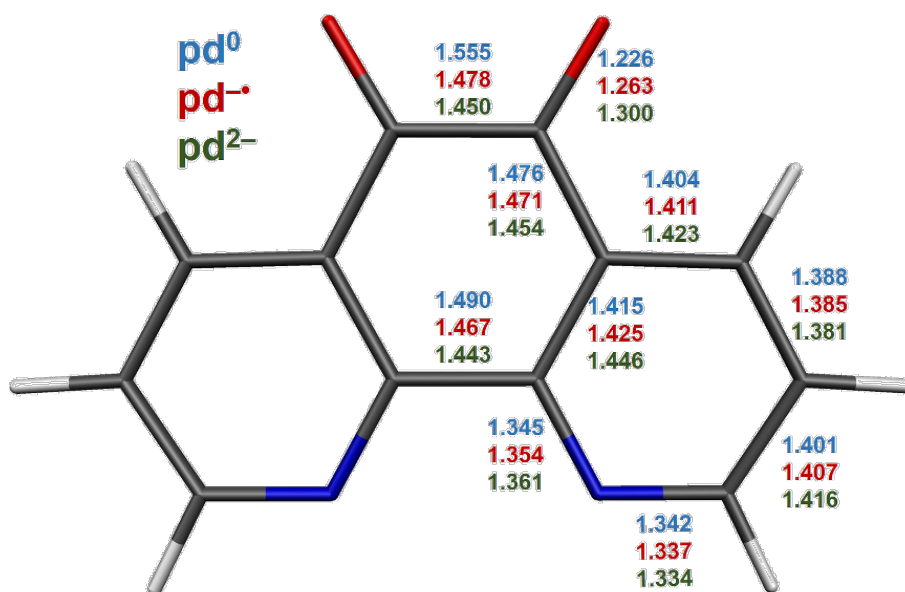


Fig. S19 Comparison of the geometry optimised bond lengths in  $[pd]^{0/1-/2-}$

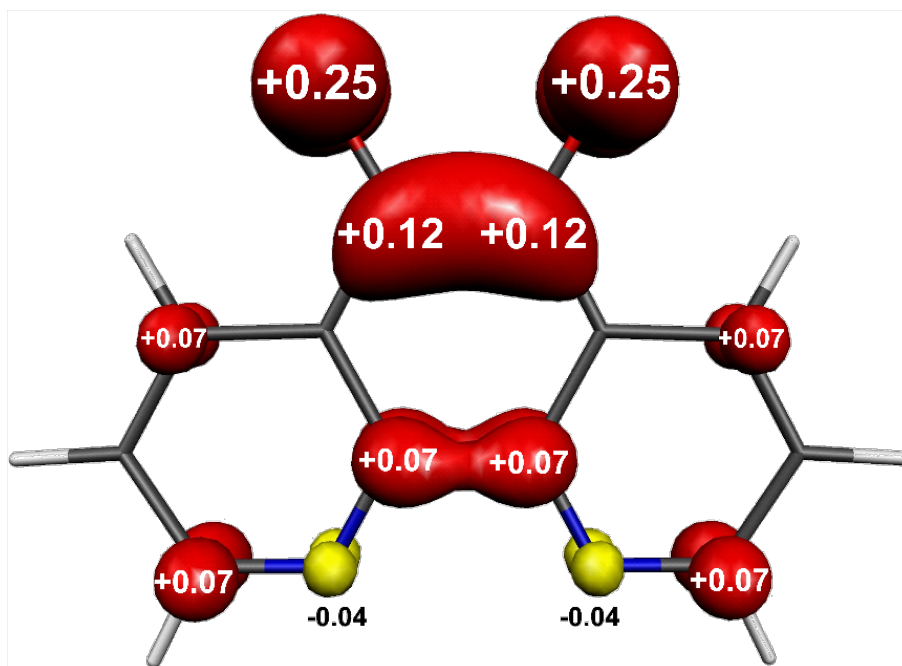
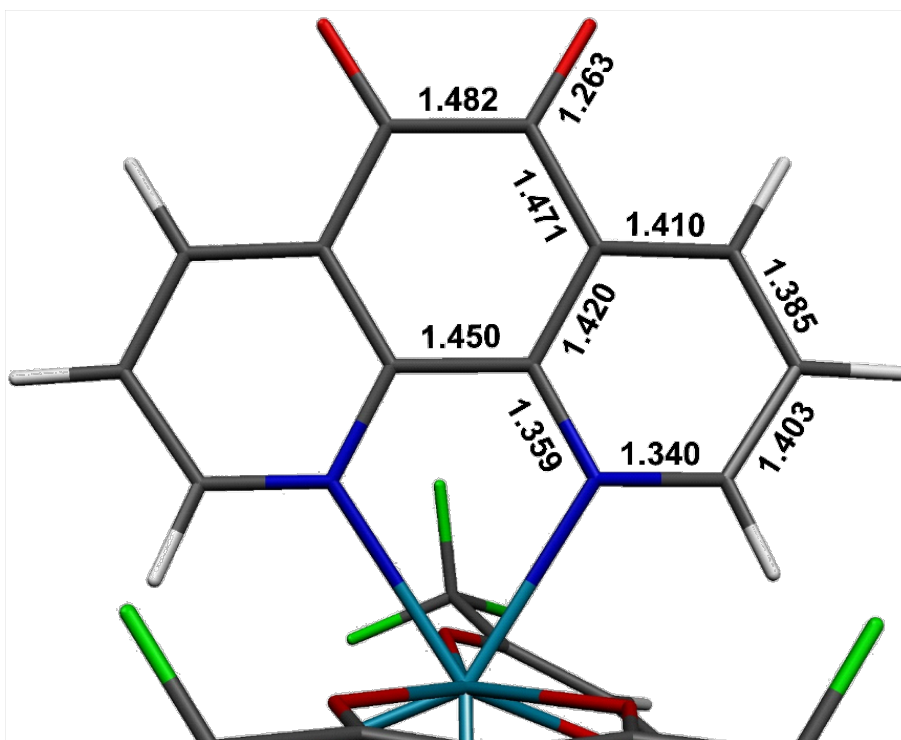
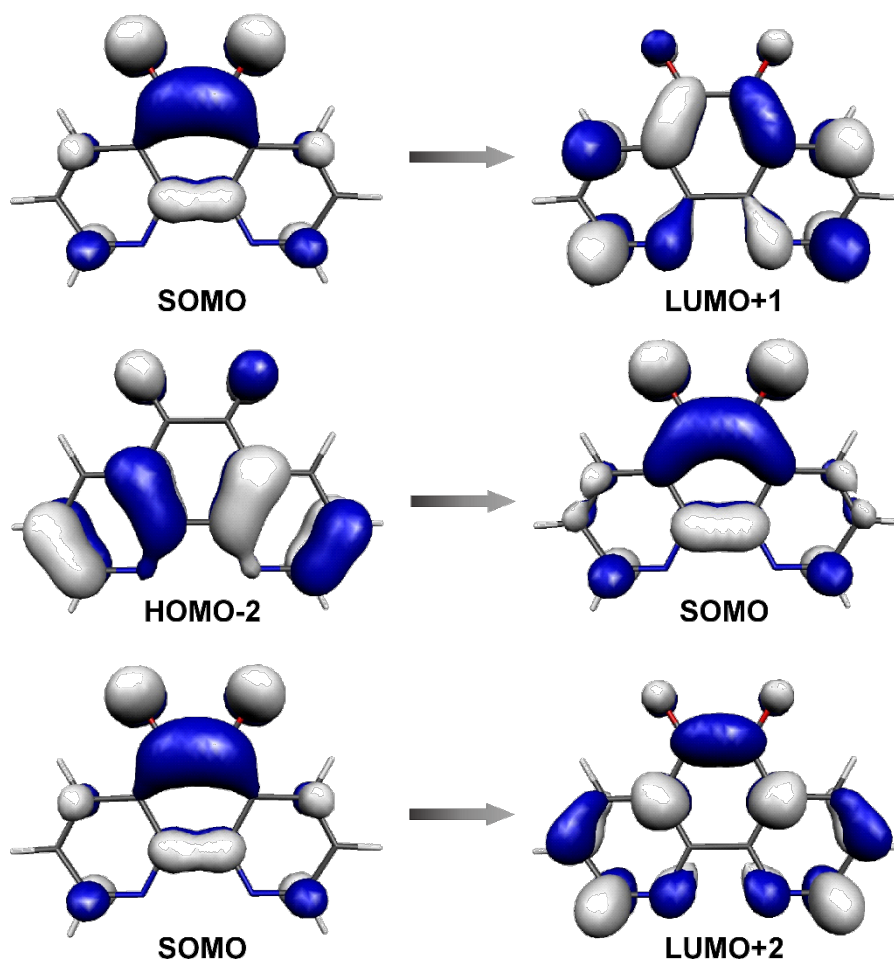


Fig. S20 Mulliken spin density plot of  $[pd]^{1-}$



**Fig. S21** Intraligand bond distances in geometry optimised  $[Y(hfac)_3(pd)]^{1-}$



**Fig. S22** Assignment of the calculated transitions at 522, 411, 364 nm, respectively, for [pd]<sup>1-</sup>

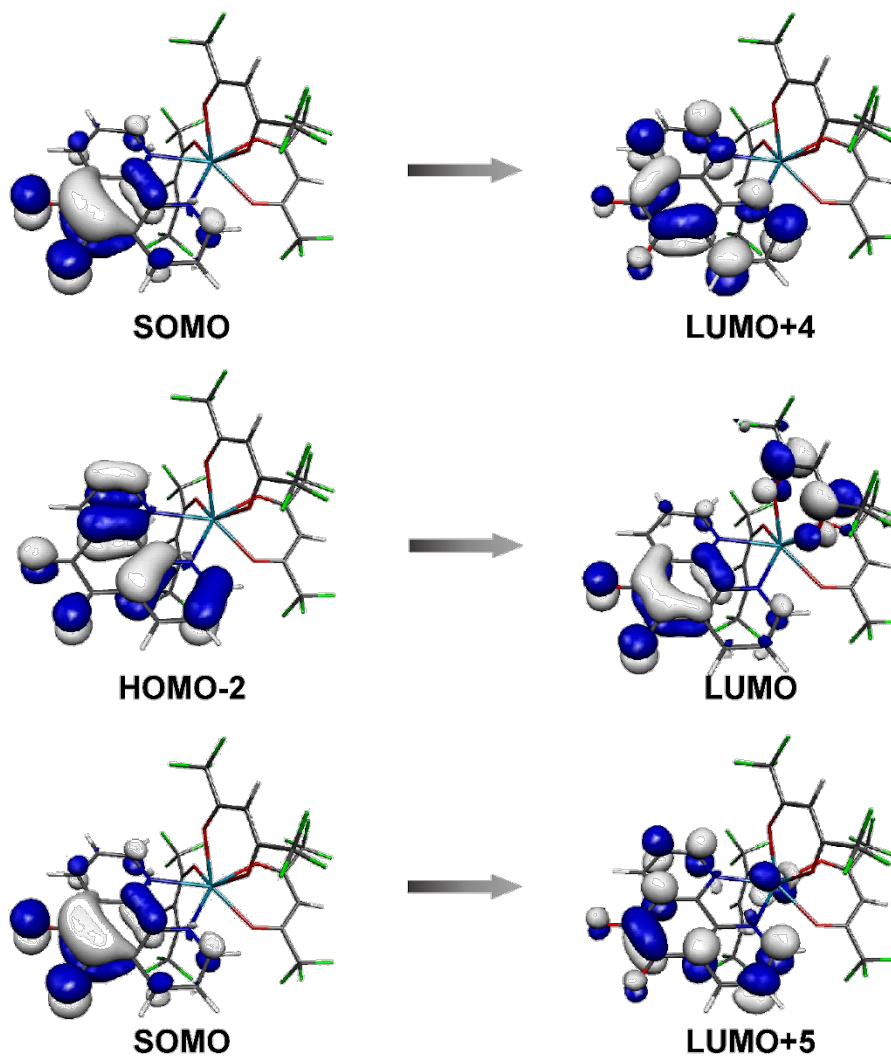


**Fig. S23** Assignment of the calculated transitions at 567, 405, 380 nm, respectively, in  $[Y(hfac)_3(pd)]^{1-}$

## References

1. H. P. Fritz, in *Adv. Organomet. Chem.*, eds. F. G. A. Stone and R. West, Academic Press, 1964, vol. 1, pp. 239-316.
2. J. R. Hickson, S. J. Horsewill, C. Bamforth, J. McGuire, C. Wilson, S. Sproules and J. H. Farnaby, *Dalton Trans.*, 2018, **47**, 10692-10701.
3. G. R. Hanson, K. E. Gates, C. J. Noble, M. Griffin, A. Mitchell and S. Benson, *J. Inorg. Biochem.*, 2004, **98**, 903-916.
4. F. Neese, *WIREs: Comp. Mol. Sci.*, 2011, **2**, 73-78.
5. A. D. Becke, *Phys. Rev. A*, 1988, **38**, 3098-3100.
6. J. P. Perdew, *Phys. Rev. B*, 1986, **33**, 8822-8824.
7. R. Ahlrichs and K. May, *Phys. Chem. Chem. Phys.*, 2000, **2**, 943.
8. F. Weigend and R. Ahlrichs, *Phys. Chem. Chem. Phys.*, 2005, **7**, 3297-3305.
9. E. van Lenthe, A. van der Avoird and P. E. S. Wormer, *J. Chem. Phys.*, 1998, **108**, 4783-4796.
10. J. H. van Lenthe, S. Faas and J. G. Snijders, *Chem. Phys. Lett.*, 2000, **328**, 107-112.
11. E. van Lenthe, J. G. Snijders and E. J. Baerends, *J. Chem. Phys.*, 1996, **105**, 6505-6516.
12. C. van Wüllen, *J. Chem. Phys.*, 1998, **109**, 392-399.
13. K. Eichkorn, O. Treutler, H. Öhm, M. Häser and R. Ahlrichs, *Chem. Phys. Lett.*, 1995, **242**, 652-660.
14. K. Eichkorn, F. Weigend, O. Treutler and R. Ahlrichs, *Theor. Chem. Acc.*, 1997, **97**, 119-124.
15. A. Klamt and G. Schuurmann, *J. Chem. Soc., Perkin Trans. 2*, 1993, 799-805.
16. P. Pulay, *Chem. Phys. Lett.*, 1980, **73**, 393-398.
17. P. Pulay, *J. Comp. Chem.*, 1982, **3**, 556-560.
18. J. P. Perdew, K. Burke and M. Ernzerhof, *Phys. Rev. Lett.*, 1996, **77**, 3865-3868.
19. C. Adamo and V. Barone, *J. Chem. Phys.*, 1999, **110**, 6158-6170.
20. D. A. Pantazis, X.-Y. Chen, C. R. Landis and F. Neese, *J. Chem. Theory Comput.*, 2008, **4**, 908-919.
21. F. Neese, F. Wennmohs and A. Hansen, *J. Chem. Phys.*, 2009, **130**, 114108.
22. R. Izsák and F. Neese, *J. Chem. Phys.*, 2011, **135**, 144105.
23. F. Neese and G. Olbrich, *Chem. Phys. Lett.*, 2002, **362**, 170-178.
24. *Molekel*, Advanced Interactive 3D-Graphics for Molecular Sciences, Swiss National Supercomputing Centre. <https://ugovaretto.github.io/molekel/>